Arch Appl Mech
DOI 10.1007/s00419-011-0541-0

ORIGINAL

Ralf Müller · Petia Dineva · Tsviatko Rangelov · Dietmar Gross

Anti-plane dynamic hole–crack interaction in a functionally graded piezoelectric media

Received: 4 January 2011 / Accepted: 29 March 2011

Abstract The anti-plane dynamic problem of a functionally graded piezoelectric plane containing a hole–crack system is treated by a non-hypersingular traction-based boundary integral equation method. The material parameters vary exponentially in the same manner in an arbitrary direction. The system is loaded by an incident SH-type wave, and impermeable boundary conditions are assumed. Using a frequency-dependent fundamental solution of the wave equation, the boundary value problem is transformed into a system of integro-differential equations along the boundary of the hole and on the crack line. Its numerical solution yields the dynamic stress intensity factors and stress concentration factors. A parametric study reveals their dependence on the hole–crack scenario and its geometry, characteristics of the dynamic load and magnitude and direction of material inhomogeneity.

Keywords Functionally graded piezoelectric material (FGPM) · Hole–crack interaction · Anti-plane deformation state · BIEM · SIFs · SCFs

1 Introduction

The stress and electric field analysis of piezoelectric solids, weakened by different type of defects such as inclusions, holes, cracks, voids, or second-phase particles, is of fundamental importance for their structural integrity and reliable service performance. Piezoelectric materials are brittle, posses low fracture resistance, and both the mechanical and electric loads are responsible for eventual catastrophic failure. Physically, the stress concentration around a hole boundary may generate cracks, and the interaction between holes and cracks may produce dielectric breakdown, damage, and fracture. Accurate prediction of the fracture response requires an accurate assessment of the interaction between the defects during service and manufacture. As a result, the interaction between holes and cracks has been a very popular topic in the field of fracture mechanics.

R. Müller
Department of Mechanical and Process Engineering, Technische Universität Kaiserslautern, 67653 Kaiserslautern, Germany

P. Dineva
Institute of Mechanics, Bulgarian Academy of Sciences, 1113 Sofia, Bulgaria

T. Rangelov (✉)
Institute of Mathematics and Informatics, Bulgarian Academy of Sciences, 1113 Sofia, Bulgaria
E-mail: rangelov@math.bas.bg
Tel.: +359(0)2-9792845
Fax: +359(0)2-9713649

D. Gross
Division of Solid Mechanics, Technische Universität Darmstadt, 64289 Darmstadt, Germany

Published online: 17 April 2011

The problems for inclusion–crack interaction are usually restricted to cases of elastic isotropic homogeneous materials under static loads. Erdogan et al. [1] studied a crack in the neighborhood of a rigid inclusion, Gharpuray et al. [2] investigated a crack emanating from a rigid inclusion, Wang and Chau [3], Hwu et al. [4] considered interactions between inclusions and various types of cracks. The interaction between a main crack and an arbitrary located elliptical hole near its tip under mode III loading conditions was solved in Gong and Meguid [5]. The boundary integral equation method (BIEM) was proposed in Liaw and Kamel [6] to evaluate the static stress intensity factors of a crack approaching a curvilinear hole in an anisotropic elastic plane. By using complex variables method and Fredholm integral equation method, the static interaction between multiple cracks and a circular hole under anti-plane deformation was studied in Chen and Wang [7]. The static interaction of an inclusion with arbitrary geometrical shape and a line crack is studied by Hasebe et al. [8] by the Green's function of a point dislocation derived for an infinite plane with an arbitrary-shaped hole. There are few results for dynamic interaction between crack and a circular hole even in the case of elastic isotropic homogeneous solid, see Lu and Hanyga [9], Meguid and Wang [10], Wang and Yu [11]. Dynamic interactions between multiple cracks and a circular hole subjected to incident SH wave have been studied in [9,10].

One of the first solutions that consider the static interaction of two circular electrically permeable holes in a piezoelectric homogeneous plane under the assumption of plane strain is presented by BIEM in Xu and Rajapakse [12]. The accuracy of the BIEM code is verified by comparison with analytical solutions for a single circular hole in a piezoelectric plane by Sosa [13] and with the solution by Lekhnitskii [14] for pure elastic anisotropic case. Liu and Fan [15] used the conventional displacement BIEM for solving a static problem of an elliptical hole with a prescribed ratio of the semiaxis a/b subjected to uniform tension. They show that the BIEM results obtained by 44 quadratic boundary elements are in excellent agreement with the exact solution for all three values of $a/b = 1; 0.5; 0.05$. When the ratio a/b is further reduced and the elliptical hole becomes an open crack, the number of elements should be increased, reaching 180 at $a/b = 0.01$. When the ratio is $a/b = 0.001$, even the 204 boundary elements cannot provide converged results because the displacement BIEM degenerates and a traction-based BIEM should be used. The BIEM analysis of the crack-hole in-plane static problem in a piezoelectric plate under external heat-flux disturbance is presented by Qin and Mai [16]. The solution is based on the termoelectroelastic Green's function for a piezoelectric solid with a hole. The same methodology is applied for inclusion–crack interaction problems of plane thermopiezoelectric solids by Qin and Lu [17]. In Zhou et al. [18], the Green's function for a piezoelectric plane with an elliptic hole with or without air is derived, and further, the hole–crack static interaction is studied by the method of singular integral equations. Numerical results show that the distribution of stress and the electric field concentration near the elliptic hole depends on the location and orientation of the crack. The dynamic interaction between a crack and a circular hole in a piezoelectric plane is investigated by Song et al. [19] by the method of complex variable and Green's function for an infinite piezoelectric plane with a single hole subjected to time-harmonic anti-plane line force.

Most of the references discussed earlier are for the static problems and for isotropic homogeneous pure elastic solids. There is a lack of results for dynamic hole–crack interaction problems even for homogeneous piezoelectrics, and to the authors' knowledge, there are no results for this problem in the case of functionally graded piezoelectric solids. In Dineva et al. [20], the authors solved a dynamic anti-plane crack problem for a functionally graded material, while in Dineva et al. [21], the similar problem was solved for a single hole. The present paper is based on the results obtained in [20,21] and investigates the dynamic interaction between hole and crack.

The main objective of this study is to evaluate stresses and electric field distribution of a hole–crack system in an inhomogeneous piezoelectric plane with exponentially varying properties in an arbitrary direction.

The paper is organized as follows: The problem statement is given in Sect. 2. Non-hypersingular traction-based BIE formulation of the posed problem is discussed in Sect. 3, and the numerical procedure is presented in Sect. 4. A series of numerical results and their interpretation is shown in Sect. 5, while some conclusions are given in Sect. 6.

2 Problem statement

In a Cartesian coordinate system $Ox_1x_2x_3$, consider an infinite, transversely isotropic functionally graded piezoelectric media with the axis of symmetry and the poling axis along Ox_3. The anti-plane deformation state is considered in the plane perpendicular to the poling axis. The plane $x_3 = 0$ contains a crack $\Gamma_{\rm cr}$ with a half-length c and a circular hole H of radius R and center C, $\partial H = \Gamma_h$ such that $\Gamma_{\rm cr} \cap \Gamma_h = \emptyset$, see Fig. 1. The

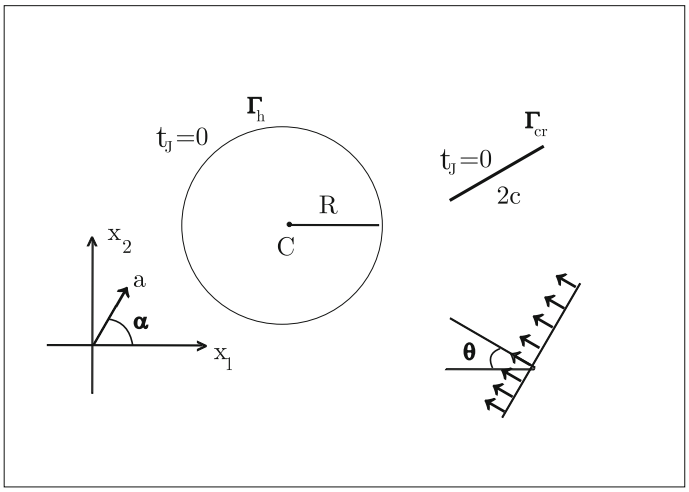

Fig. 1 A hole–crack system in a functionally graded piezoelectric plane under SH-type wave

direction of the incident time-harmonic shear wave with a circular frequency ω is given by the angle θ with respect to the x_1 axis. Because of the time-harmonic behavior of all field quantities, the common multiplier $e^{i\omega t}$ is suppressed here and in the following. The only non-vanishing displacements are the anti-plane mechanical displacement $u_3(x,\omega)$ and the in-plane electrical displacements $D_i(x,\omega)$, while the non-vanishing stress components are $\sigma_{i3}(x,\omega)$, $i=1,2$, $x=(x_1,x_2)$. The incident wave interacts with the hole–crack system and produces scattered wave, so that the total wave field is a superposition of the incident and scattered waves. The decomposition $u_3(x,\omega) = u_3^{in}(x,\omega) + u_3^{sc}(x,\omega)$ for the displacement holds analogously for all field quantities. The boundary value problem for the scattered wave field is formulated as follows:

In absence of volume forces and electric charges, the balance equations are given by

$$\sigma_{i3,i} + \rho\omega^2 u_3 = 0, \qquad D_{i,i} = 0 \tag{1}$$

The strain–displacement and electric field–potential relations are

$$s_{i3} = u_{3,i}, \quad E_i = -\phi_{,i} \tag{2}$$

and the constitutive equations read

$$\begin{aligned} \sigma_{13} &= c_{44}s_{13} - e_{15}E_1, \\ \sigma_{23} &= c_{44}s_{23} - e_{15}E_2, \\ D_1 &= e_{15}s_{13} + \varepsilon_{11}E_1, \\ D_2 &= e_{15}s_{23} + \varepsilon_{11}E_2. \end{aligned} \tag{3}$$

Here, s_{i3}, E_i, ϕ are the strain tensor, the electric field vector, and the electric potential, respectively, $i=1,2$, subscript commas denote partial differentiation and the summation convention for repeated indices is applied.

We assume that all material parameters, i.e. the mass density ρ, the shear stiffness c_{44}, the piezoelectric e_{15}, and the dielectric permittivity ε_{11}, vary in the same manner exponentially with x:

$$c_{44} = c_{44}^0 e^{2<a,x>}, \quad e_{15} = e_{15}^0 e^{2<a,x>}, \quad \varepsilon_{11} = \varepsilon_{11}^0 e^{2<a,x>}, \quad \rho = \rho^0 e^{2<a,x>} \tag{4}$$

where $<,>$ denotes the scalar product in R^2. Here, c_{44}^0, e_{15}^0, ε_{11}^0, ρ^0 are reference material constants, e.g. the material characteristics in the homogeneous case.

The crack's line and the hole's boundary are assumed to be free of both mechanical traction and surface charges, i.e. an impermeable crack and hole are considered:

$$t_3 = \sigma_{i3}n_i = 0, \qquad D_i n_i = 0 \quad \text{on} \quad \Gamma = \Gamma_{\text{cr}} \cup \Gamma_h, \tag{5}$$

where n_i are the components of the outward normal vector in every point of Γ.

Using the notation by Davi and Milazzo [22] where $u_J = (u_3, \phi)$, $J = 3, 4$; $s_{iJ} = \begin{cases} s_{i3}, J = 3 \\ E_i, J = 4 \end{cases}$, $\sigma_{iJ} = \begin{cases} \sigma_{i3}, J = 3 \\ D_i, J = 4 \end{cases}$ and $t_J = \sigma_{iJ} n_i$ are the generalized displacement, strain, stress, and traction, respectively; Eqs. (1)–(3) can be written in the compact form

$$\sigma_{iJ,i} + \rho_{JK} \omega^2 u_K = 0, \quad J, K = 3, 4 \tag{6}$$

where $\rho_{JK} = \begin{cases} \rho, J = K = 3, \\ 0, J = 4 \text{ or } K = 4. \end{cases}$ Using the generalized stiffness tensor

$$C_{i33l} = \begin{cases} c_{44}, i = l \\ 0, \quad i \neq l \end{cases}, \quad C_{i43l} = C_{i34l} = \begin{cases} e_{15}, i = l \\ 0, \quad i \neq l \end{cases}, \quad C_{i44l} = \begin{cases} -\varepsilon_{11}, i = l \\ 0, \quad i \neq l \end{cases}$$

the generalized stress is $\sigma_{iJ} = C_{iJKl} u_{K,l}$.

The boundary condition Eq. (5) for the total traction on the crack or on the boundary of the hole takes the following form

$$t_J(x, \omega) = 0 \quad \text{on } \Gamma. \tag{7}$$

The wave scattered by the hole–crack system in a functionally graded piezoelectric plane is governed by partial differential Eq. (6) with variable coefficients. Following the approach proposed in [23], the smooth transform is applied to the displacement vector $u_J(x, \omega)$

$$u_J(x, \omega) = e^{-<a,x>} U_J(x, \omega). \tag{8}$$

The following system of partial differential equations with constant coefficients for the displacement vector $U_J(x, \omega)$ is obtained

$$C^0_{iJKl} U_{K,il} + \left(\rho^0_{JK} \omega^2 - C^0_{iJKi} |a|^2\right) \; U_K = 0. \tag{9}$$

Replacing the displacement component U_4 from the second equation in the system of equations (9) into the first one, the following equation for the mechanical displacement U_3 is obtained

$$U_{3,ii} + k^2 U_3 = 0. \tag{10}$$

where $k^2 = \frac{\rho^0}{a_0}\omega^2 - |a|^2$, $a_0 = c^0_{44} + \frac{e^{02}_{15}}{\varepsilon^0_{11}}$. Denote by $\omega_0 = \sqrt{\frac{a_0}{\rho^0}}|a|$ and consider the following cases with respect to the frequency ω:

(a) the case $\omega > \omega_0$, where we have that $k^2 > 0$ which corresponds to the case of a wave propagation process;
(b) the case that $\omega = \omega_0$, where we have that $k^2 = 0$ and no wave propagation occurs; the behavior of the solution is as in the static case;
(c) the case $\omega < \omega_0$, where we have that $k^2 < 0$ which is the case of simple vibration.

The type of the dynamic behavior of the hole–crack system is governed by the frequency of the incident wave and the material properties of the inhomogeneous piezoelectric material. In this work, we assume that the frequency of the incident wave fulfills the case (a).

Furthermore, suppose that $U_J(x, \omega)$ in Eq. (8) satisfies Sommerfeld-type condition at infinity, more specifically

$$U_3 = o(|x|^{-1}), U_4 = o(e^{-|a||x|}) \quad \text{for} \quad |x| \to \infty. \tag{11}$$

Condition (11) ensures uniqueness of the scattering wave field u^{sc}_J for a given incident wave u^{in}_J. Following Akamatsu and Nakamura [24], it can be proved that the boundary value problem (BVP) given by Eqs. (6), (7) in conjunction with condition (11) admits a continuous differentiable solution.

The displacement and the traction field of the incident SH wave is a solution of equation (6). This solution is obtained by the use of the smooth functional transform (8) and solution of Eq. (9) obtained by plane wave

decomposition technique. For a plane SH wave with an incident direction $\xi = (\xi_1, \xi_2)$, the displacement field at a given frequency ω and at an observer point x is as follows:

$$\begin{aligned} u_3^{in}(x,\omega) &= e^{-<x,a+ik\xi>} \\ u_4^{in}(x,\omega) &= \frac{e_{15}^0}{\varepsilon_{11}^0} u_3(x,\omega). \end{aligned} \tag{12}$$

The corresponding traction field on Γ is

$$\begin{aligned} t_3^{in}(x,\omega) &= -a_0 < n, a + ik\xi > e^{<x,a-ik\xi>} \\ t_4^{in} &= 0. \end{aligned} \tag{13}$$

3 BIEM formulation and fundamental solution

The boundary value problem posed in sect. 2 and consisting of Eqs. (6), (7), and (11) can be formulated by a system of traction boundary integral equations on Γ using the representation formulas for the piezoelectric continua, see [25,26], and the non-hypersingular traction BIEM proposed by Zhang and Gross [27] for the pure elastic solid. For the considered problem, it is a combination of the BIEM numerical schemes given in Dineva et al. [20,21]:

$$\begin{aligned} c_J(x) t_J^{in}(x) = C_{iJKl}(x) n_i(x) \int_{\Gamma_h} & \big[(\sigma^*_{\eta PK}(x,y,\omega) u_{P,\eta}(y,\omega) \\ & - \rho_{QP}\omega^2 u^*_{QK}(x,y,\omega) u_P(y,\omega)) \delta_{\lambda l} - \sigma^*_{\lambda PK}(x,y,\omega) u_{P,l}(y,\omega) \big] n_\lambda(y) dS_h \\ & - C_{iJKl}(x) n_i(x) \int_{\Gamma_h} u^*_{PK,l}(x,y,\omega) t_P^{in}(y,\omega) \mathrm{dS_h} \\ & + C_{iJKl}(x) n_i(x) \int_{\Gamma_{cr}} [(\sigma^*_{\eta PK}(x,y,\omega) \Delta u_{P,\eta}(y,\omega) - \rho_{QP}\omega^2 u^*_{QK}(x,y,\omega) \Delta u_P(y,\omega)) \delta_{\lambda l} \\ & - \sigma^*_{\lambda PK}(x,y,\omega) \Delta u_{P,l}(y,\omega)] n_\lambda(y) \mathrm{dS_{cr}}, \quad \mathrm{x} \in \Gamma. \end{aligned} \tag{14}$$

where $c_J(x) = \begin{cases} -1/2, & x \in \Gamma_h \\ -1, & x \in \Gamma_{\mathrm{cr}} \end{cases}$, u^*_{QK} is the fundamental solution of (6), $\sigma^*_{iJQ} = C_{iJKl} u^*_{KQ,l}$ is the corresponding stress and $\Delta u_J = u_J|_{\Gamma^+_{\mathrm{cr}}} - u_J|_{\Gamma^-_{\mathrm{cr}}}$ is the generalized crack opening displacement (COD) of the crack Γ_{cr}. Furthermore, x and y denote the position vectors of the field and source point, respectively.

For u_J, u^*_{JK}, we apply Green's formula in the domain $\Omega_R \backslash (\Omega^{\mathrm{cr}}_\varepsilon \cup \Omega^h_\varepsilon)$, where Ω_R is a circular domain with large radius R, $\Omega^{\mathrm{cr}}_\varepsilon$ is a small neighborhood of the crack and Ω^h_ε is a small neighborhood of the hole. Applying the representation formulae for the generalized displacement gradient $u_{K,l}$, see Wang and Zhang [28], an integro-differential equation on $\partial\Omega_R \cup \partial\Omega^{\mathrm{cr}}_\varepsilon \cup \partial\Omega^h_\varepsilon$ is obtained. Using the condition (11) the integrals over $\partial\Omega_R$ go to 0 for $R \to \infty$. Taking the limit $\varepsilon \to 0$, i.e. $x \to \Gamma$ and using the boundary condition (6), i.e. $t_J^{sc} = -t_J^{in}$ on Γ, the system of non-hypersingular traction BIE (14) is obtained and it is equivalent to the BVP defined by the Eqs. (5) and (6).

Equation (14) forms a system of integro-differential equations with respect to the unknown displacement u_J along the boundary of the hole Γ_h and to the crack opening displacement Δu_J on the crack line Γ_{cr}. The generalized displacement and traction of the scattered wave field at each point in the smoothly inhomogeneous piezoelectric plane can be determined by using the corresponding representation formulae, see [21,23], and the solutions of Eq. (14).

In order to solve Eq. (14), it is necessary to know the fundamental solutions for displacement and traction and their derivatives. The fundamental solution of (6) is defined as solution of the equation

$$\sigma^*_{iJM,i} + \rho_{JK}\omega^2 u^*_{KM} = -\delta_{JM}\delta(x,\xi), \tag{15}$$

where $x = (x_1, x_2)$, $\xi = (\xi_1, \xi_2)$, δ is Dirac's function, and δ_{JM} is the Kronecker symbol. The derivation of the fundamental solution was presented and discussed in [23], see also [21].

4 Numerical procedure

The numerical procedure for solution of the posed BVP follows the numerical algorithm developed and validated by Rangelov et al. [23], Dineva et al. [21]. The hole boundary Γ_h and the crack $\Gamma_{\rm cr}$ are discretized by quadratic boundary elements (BE) away from the crack tips and special crack-tip quarter-point BE near the crack tips to model the asymptotic behavior of the displacement and traction. Applying the shifted point scheme, the singular integrals converge in Cauchy principal value (CPV) sense, since the smoothness requirements $\Delta u_J \in C^{1+\alpha}(\Gamma_{\rm cr})$, $u_J \in C^{1+\alpha}(\Gamma_h)$, $t_J \in C^{\alpha}(\Gamma)$ of the approximation are fulfilled, see Rangelov et al. [29]. Due to the form of the fundamental solution as an integral over the unit circle, see Appendix A in [20], and all integrals in Eq. (14) are two dimensional.

After discretization procedure of the BIE, solution of all type of integrals, see Appendix B in [20], and satisfying the boundary conditions, an algebraic system of equations for the crack opening displacement Δu_J along the crack $\Gamma_{\rm cr}$ and displacement u_J along the hole boundary Γ_h is obtained and solved. Following this procedure, a program code based on Mathematica and FORTRAN has been created.

The most essential quantities that characterize the mechanical and electric field concentrations are SIFs and SCFs. Following Pao and Mow [30]; Manolis and Beskos [31] for pure elastic case, and Fang [32]; Shindo et al. [33] for the piezoelectric case, the dynamic SCF and electric field concentration factor (EFCF) along the perimeter of a circular hole are defined as the ratio of the stress and electric field along the circumference to the maximum amplitude of the incident stress at the same point, see [21]. The normalized dynamic SCF $|\sigma_{\gamma\theta}/\tau_0|$ and the normalized dynamic EFCF $|e_{15}E_{\gamma\theta}/\tau_0|$ are calculated by using the following formulae:

$$\begin{aligned}
\sigma_{\theta\gamma} &= -\sigma_1 \sin(\theta-\gamma) + \sigma_2 \cos(\theta-\gamma),\\
\sigma_i &= \sigma_{i3} + \sigma_{i3}^{in},\\
E_{\theta\gamma} &= -E_1 \sin(\theta-\gamma) + E_2 \cos(\theta-\gamma),\\
E_i &= \frac{e_{15}^0}{e_{15}^{02} + c_{44}^0 \varepsilon_{11}^0}\left(-e_{15}^0 \sigma_i + c_{44}^0 D_i\right),\\
D_i &= \sigma_{i4} + \sigma_{i4}^{in}.
\end{aligned} \tag{16}$$

Here, τ_0 is the amplitude of the maximal shear stress of the incident SH wave, i.e. $\tau_0 = i\omega\sqrt{a_0\rho^0}$, γ is the angle of the observation point, θ is the incident wave angle and a_0 is defined in section 2.

The dynamic mechanical SIF K_{III} and the electrical displacement intensity factor K_D are obtained directly from the nodal traction values ahead of the crack tip, see Suo et al. [34]. In case of a straight crack along the interval $(-c, c)$ on the Ox_1 axis, they are defined as

$$K_{III} = \lim_{x_1 \to \pm c} t_3 \sqrt{2\pi(x_1 \mp c)}, \quad K_D = \lim_{x_1 \to \pm c} t_4 \sqrt{2\pi(x_1 \mp c)}, \tag{17}$$

where t_J is the generalized traction at the point $(x_1, 0)$ close to the crack tip.

5 Results

In all examples, the crack length is $2c = 5$ mm and the crack is discretisized by 7 BE. The first and the last BE are quarter-point BE, while the remaining elements are ordinary quadratic BE. Their lengths l_j are chosen as follows: $l_1 = l_7 = 0.375\,\text{mm}$, $l_2 = l_6 = 0.5\,\text{mm}$, $l_3 = l_5 = 1.0\,\text{mm}$, $l_4 = 1.25\,\text{mm}$. The hole has the radius $R = 5\,\text{mm}$, and its boundary is discretisized by 14 ordinary quadratic BE.

There are in general two cases for mutual dispositions of the circular hole and finite straight line crack: (a) The crack ligament intersects the hole; (b) The crack line does not intersect the hole. For the simulation studies we will use, just for simplicity the particular cases shortly quoted in what follows as: hole–horizontal crack configuration, as shown in Fig. 2a and the ligament of the crack pass through the center C of the hole; hole–vertical crack configuration, as shown in Fig. 2b and the line through the center of the hole and the center of the crack is perpendicular to the crack.

The inhomogeneity parameter $a = (a_1, a_2)$ in the inhomogeneity function $e^{2<a,x>}$ is written in polar coordinates as $a = r(\cos\alpha, \sin\alpha)$ where α and r are the direction and the magnitude of the material gradient. To the best of the authors' knowledge, there are no SIF and SCF results available for a hole–crack system in a piezoelectric plane with exponentially varying material properties subjected to time-harmonic SH-type wave.

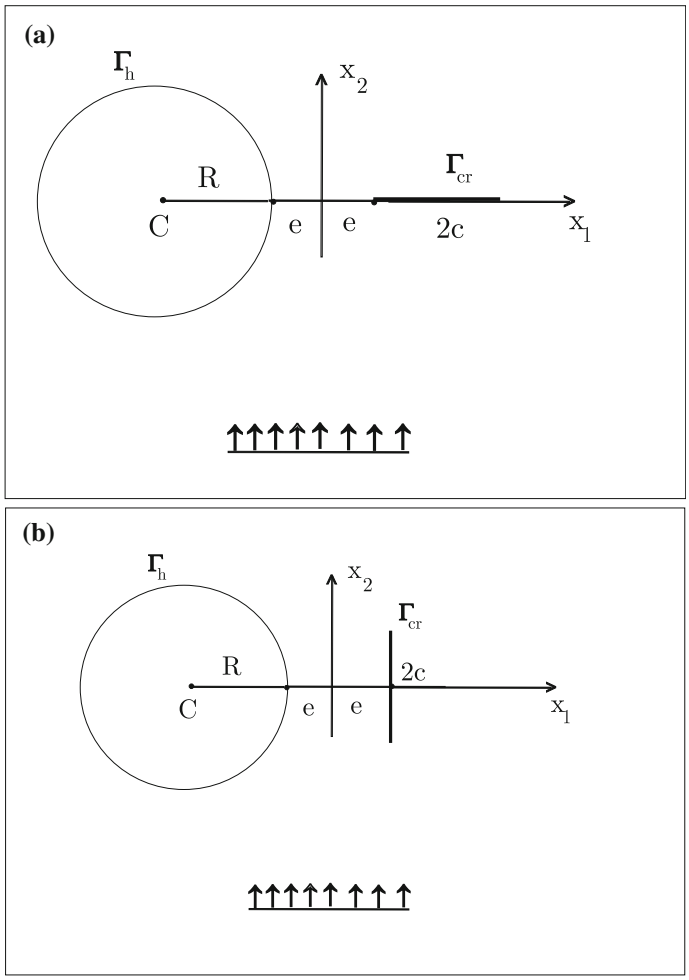

Fig. 2 The configurations of the hole–crack systems in numerical examples

For this reason the validation of the numerical scheme is possible only by comparing the authors' BIEM results with results of other authors for the homogeneous case. For this purpose the magnitude of the inhomogeneity gradient r in the developed program code is simply set to 0.

5.1 Validation study

The proposed numerical procedure is validated by solution of two benchmark problems. The first test example considers an infinite homogeneous plane containing a circular hole with radius R and center $C(-e - R, 0)$ and a crack along the segment $(e, e + 2c)$ on the Ox_1 axis subjected to SH wave directed at an incident angle θ with respect to Ox_1 axis, see Fig. 2a. To the best of the authors' knowledge, the only results for this problem are published by Song et al. [19]. The solution is obtained by the complex variable method based on Green's function for a single hole in a piezoelectric plane. The second benchmark example considers the first one but in the case the distance $d = 2e$ between the hole and the crack is 10 times the half-length of the crack c. In this case, the computed SIFs coincide with the results obtained by: (a) Wang and Meguid [35] who studied a homogeneous piezoelectric plane with a single crack; (b) Daros [36] who used non-hyper-singular traction BIEM to solve the same problem in the case of an exponential inhomogeneous anisotropic plane. In the second test example, the SCFs along the boundary of the hole coincide with the results obtained by Shindo et al. [33] for a single circular hole in a homogeneous piezoelectric plane under incident SH wave.

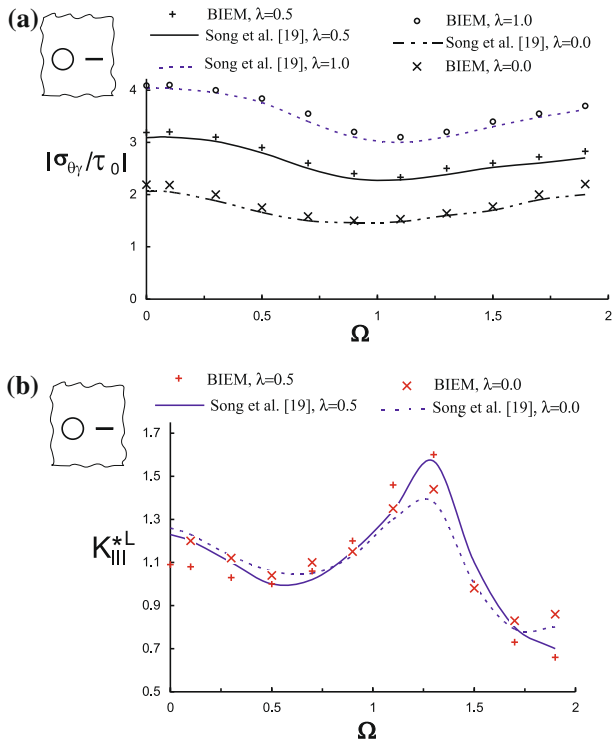

Fig. 3 SCF and SIF for a hole–horizontal crack system versus normalized frequency Ω of normal incident SH wave propagating in a homogeneous piezoelectric plane: **a** SCF at observer point $\gamma = 0$; **b** K^{*L}_{III}

Figure 3a shows a comparison of the results for the SCF versus the normalized frequency $\Omega = c\sqrt{\rho^0/c^0_{44}}\omega$ at the observation point $A(-e, 0)$, i.e. $\gamma = 0$, obtained by the proposed method and by the complex variable method proposed by Song et al. [19]. For this case, the following data are used as follows: $R = c = e$, $C = (-2e, 0)$, and $d = 2e$. Piezoelectric materials with different values of the coefficient $\lambda = \frac{e^{02}_{15}}{c^0_{44}\varepsilon^0_{11}}$ are considered as follows: $\lambda = 0.5$, $\lambda = 1.0$, and $\lambda = 0$ for the case of isotropic material. The reference constants for PZT-4 are $c^0_{44} = 2.56 \times 10^{10}\mathrm{N/m^2}$, $e^0_{15} = 12.7\mathrm{C/m^2}$, $\varepsilon^0_{11} = 64.6 \times 10^{-10}\mathrm{C/Vm}$, $\rho^0 = 7.5 \times 10^3\mathrm{kg/m^3}$. The prescribed values of λ are obtained by variation of e^0_{15}. The incident wave angle is $\theta = \pi/2$. Figure 3b shows the normalized dynamic SIF $K^*_{III} = |K_{III}/\tau_0\sqrt{\pi c}|$ at the left crack tip for $\lambda = 0.5$, $\lambda = 0.0$. As can be seen, the BIEM results agree very well with those by Song et al. [19].

Figure 4 presents results for mechanical SCF and electrical field concentration factor EFCF versus normalized frequency Ω for the same hole–crack scenario as those in Fig. 2a but for the case that the distance between the hole and the crack is $d = 10c$. At this distance, the hole–crack interaction is very weak and the solution for the hole–crack system recovers the solutions for the single hole and the single crack. In Fig. 4a and b, the solutions are compared with the ones obtained by the proposed method for two different boundary value problems in a piezoelectric PZT-4 homogeneous plane subjected to normal SH wave: (a) a single anti-plane crack and (b) a system of hole–crack. Both solutions are almost identical. An additional comparison is done with solution obtained by Shindo et al. [33] for a single circular hole. The difference between three results is very small, less than 8%. This indicates a high accuracy and convergence of the proposed numerical scheme in the considered frequency interval.

Figure 5 shows SIF K^*_{III} at the left crack tip of a crack from a hole–crack configuration given in Fig.2a. The distance between the hole and the crack is $d = 10c$. The authors' solutions for both a single anti-plane crack and a hole–crack system in a homogeneous piezoelectric plane are very close. This is true also for inhomogeneous piezoelectric plane with normalized magnitude $r = 0.2/c$ and inhomogeneity direction $\alpha = 0$, where the authors' results obtained by the non-hypersingular traction BIEM are very close to the solution obtained by Daros [36]. For the homogeneous case, all three solutions are very close. For the inhomogeneous case, the authors' results are slightly higher by 7–9% than the solutions in [36].

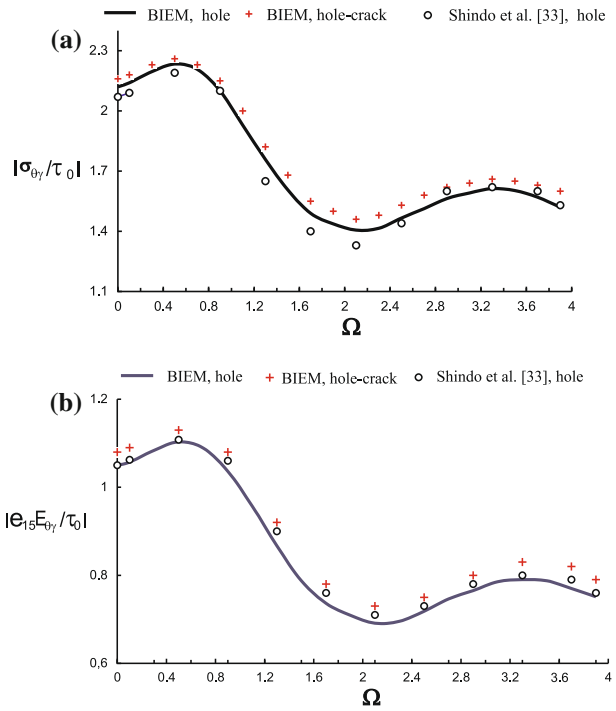

Fig. 4 SCF at observer point $\gamma = 0$ versus normalized frequency Ω of normal incident SH wave propagating in a homogeneous piezoelectric plane: **a** hole; **b** hole–horizontal crack system at distance $d = 10c$

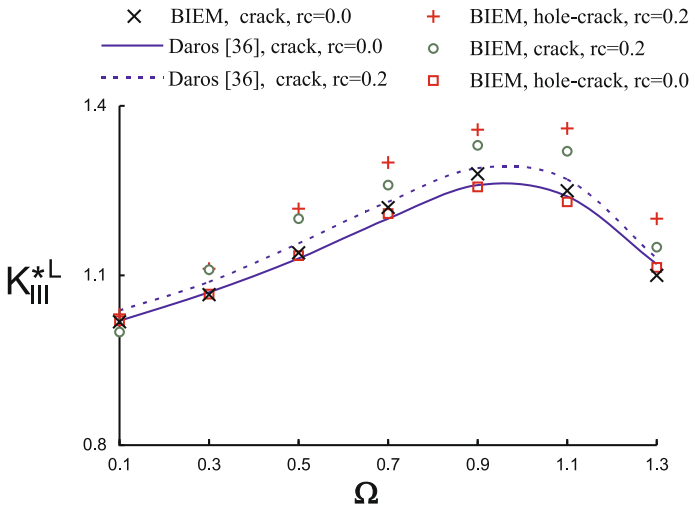

Fig. 5 K^{*L}_{III} for a system hole–horizontal crack at $d = 10c$ vs. normalized frequency of normal incident SH-type wave propagating in an exponentially inhomogeneous piezoelectric plane

5.2 Simulation results

The aim of the simulation study is to provide some insight into the effect of various system parameters on the stress and electric field concentrations. These parameters are as follows: (a) the frequency and incident angle of the applied load, (b) the direction α and magnitude r of the material inhomogeneity, (c) the electro-mechanical coupling, (d) the wave–hole–crack and wave–material interaction, and (e) the geometry and type of the hole–crack scenario.

Figure 6 shows dynamic stress concentration fields in a system hole–horizontal crack subjected to normal incident SH wave propagating in a homogeneous piezoelectric plane with normalized frequency Ω in the

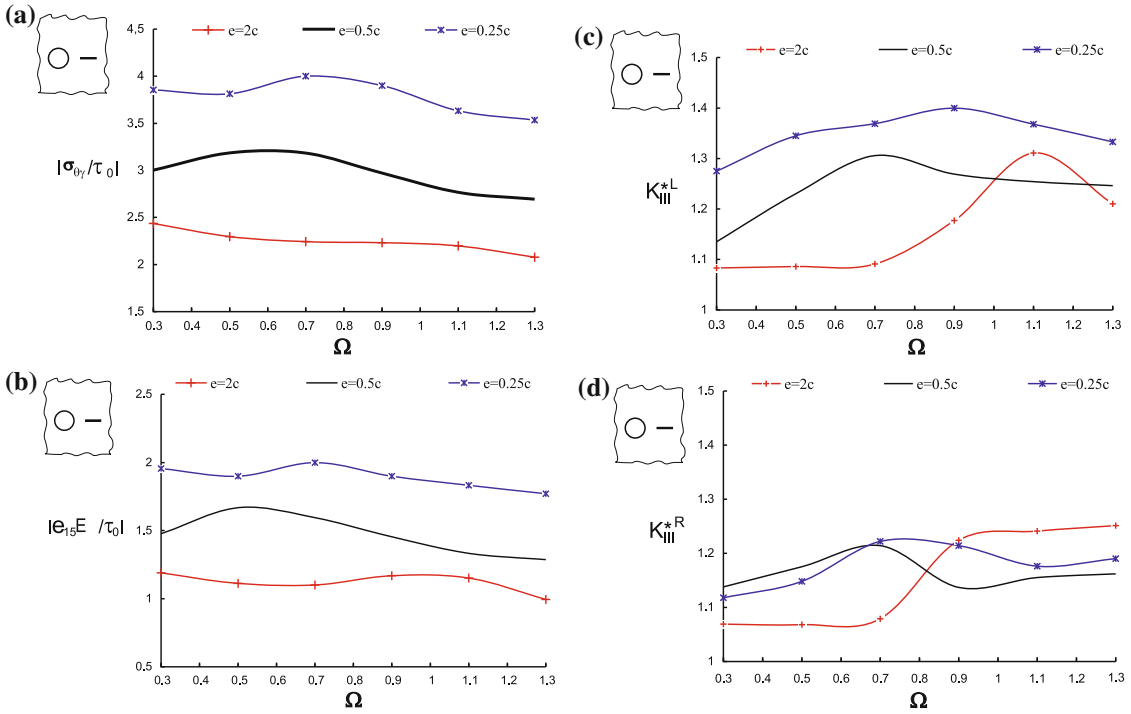

Fig. 6 Dynamic SCF and dynamic SIF vs. normalized frequency Ω of normal incident plane SH wave propagating in homogeneous piezoelectric plane with a hole–horizontal crack system as in Fig. 2a for different half-distances between hole and crack: **a** and **b** mechanical and electric field SCF at observer point $\gamma = 0$; **c** K^{*L}_{III} **d** K^{*R}_{III}

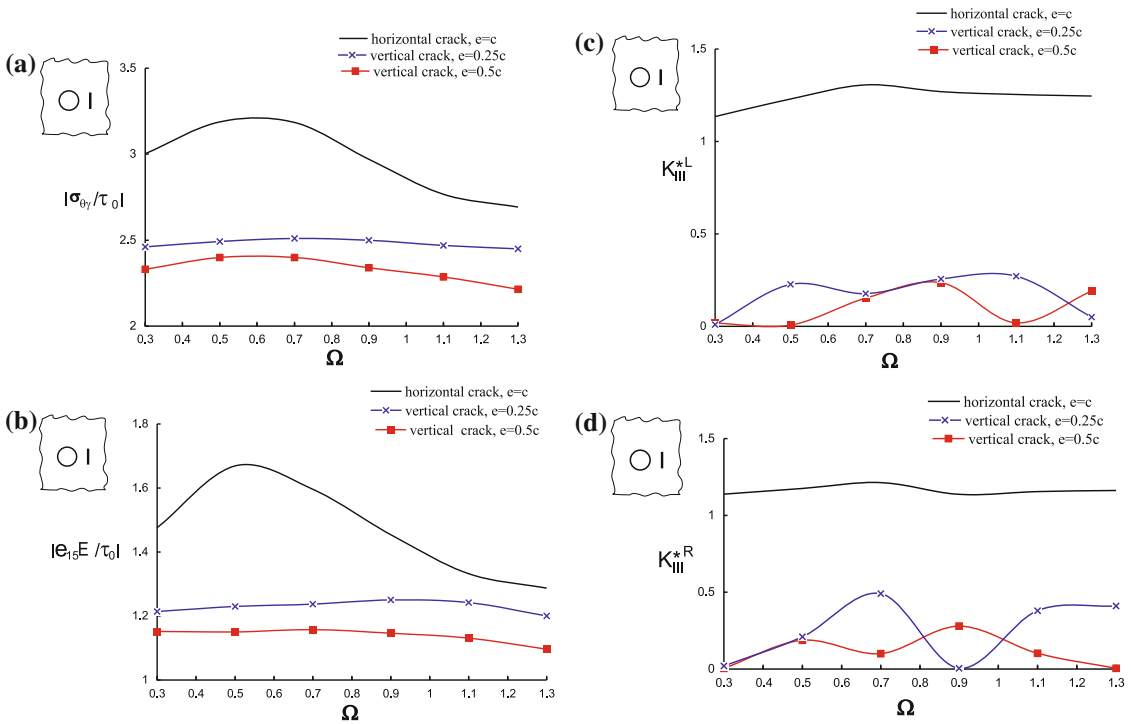

Fig. 7 Dynamic SCF and SIF vs. normalized frequency Ω of normal incident plane SH wave propagating in homogeneous piezoelectric plane with a hole–vertical crack system for different half-distances between hole and crack: **a** and **b** mechanical and electric field SCF at observer point $\gamma = 0$; **c** K^{*L}_{III} d K^{*R}_{III}

interval [0.3, 1.3]. In the hole-horizontal crack configuration (see Fig. 2a), the following cases for the half-distance between the hole and the crack are considered as follows: $e = 2c$, $e = 0.5c$, and $e = 0.25c$. Figure 6a and b for the mechanical stress and electric field concentration factors at observer point $A(-e, 0)$, i.e. $\gamma = 0$, clearly demonstrate that the stress concentration field along the hole boundary is higher when the crack is closer. As an illustration, for example at the normalized frequency $\Omega = 0.9$, the difference between mechanical and electrical stress concentration factors at hole–horizontal crack configuration with $e = 2c$ and $e = 0.25c$ is 74.8 and 62.6%, correspondingly. Figure 6c and d reveal the effect of the hole–crack geometry on the stress intensity factors K_{III}^{*L} at the left crack tip and K_{III}^{*R} at the right crack tip. This effect is stronger for the left crack tip which is closer to the hole, while at the right crack tip the effect of hole–crack interaction is weaker.

The numerical results in Fig. 7 concern the hole–vertical crack configuration (see Fig. 2b) for two values of the half-distance between the hole and the crack: $e = 0.5c$ and $e = 0.25c$. The incident angle of the SH wave is $\theta = \pi/2$, and the piezoelectric plane is homogeneous. The results for hole–vertical crack configuration are compared with the results for the hole–horizontal crack configuration. The following conclusions can be made as follows: (a) Dynamic stress concentration field near the defects expressed by the stress concentration factors along the hole's boundary and stress intensity factors near the crack tips are reduced significantly when the crack is vertical. As an illustration, for example at the normalized frequency $\Omega = 0.7$, the SCF is decreased by 32.6 and 26.8% in the case of vertical crack with half-distance between hole and crack of $e = 0.5c$ and $e = 0.25c$, respectively. Figure 7c and d show that SIF are reduced strongly in the case of vertical crack. The configuration hole–vertical crack produces reduced stress concentration field in comparison with the case of horizontal crack; (b) The sensitivity of the stress field to the half-distance e is greater in the case of horizontal crack, see Fig. 7a and b.

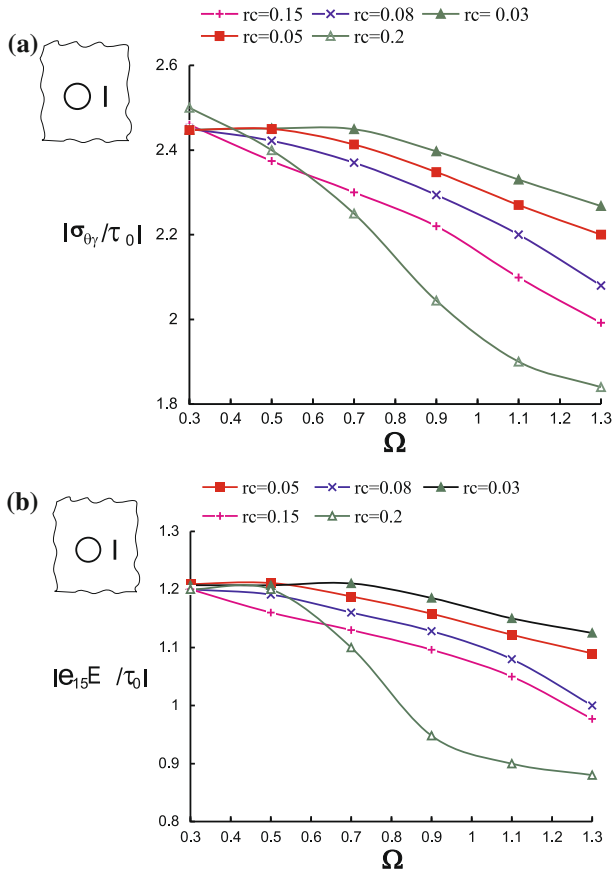

Fig. 8 Dynamic SCF at observer point $\gamma = 0$ versus normalized frequency Ω of normal incident SH-type wave propagating in inhomogeneous piezoelectric plane with inhomogeneity direction $\alpha = \pi/2$ for different magnitude rc and with a hole–vertical crack system at $e = 3.5c$: **a** mechanical SCF; **b** electric SCF

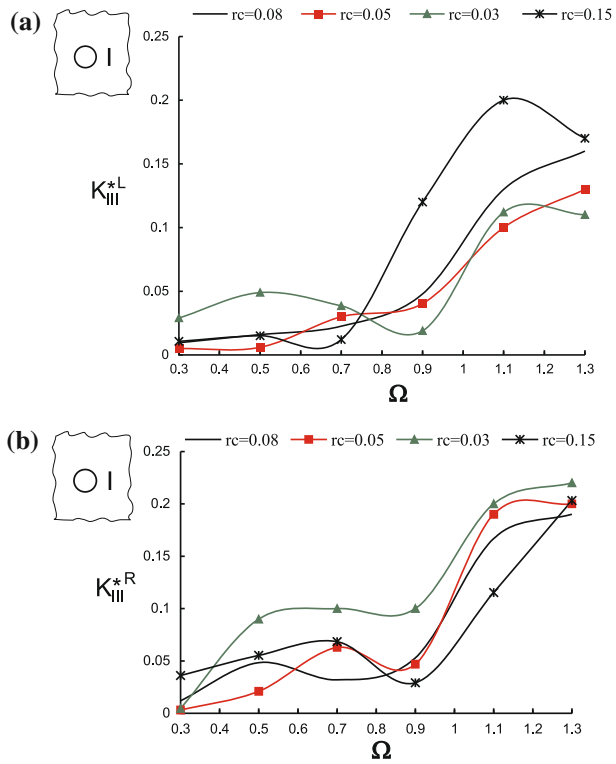

Fig. 9 Dynamic SIF versus normalized frequency Ω of normal incident SH-type wave propagating in inhomogeneous piezoelectric plane with inhomogeneity direction $\alpha = \pi/2$ for different magnitude rc and with a hole–vertical crack system at $e = 3.5c$: **a** K^{*L}_{III}; **b** K^{*R}_{III}

The aim of the following simulations is to investigate the influence of the material inhomogeneity on the stress field and its interplay with other parameters as geometry of the defect, hole–crack configuration, distance between defects, incident wave angle, and defect interaction.

Figure 8a and b demonstrate that the mechanical and the electrical stress concentration factors at observer point with $\gamma = 0$ along the circular hole (see Fig. 2b) and at half-distance between the hole and the crack $e = 3.5c$ depend strongly on the normalized frequency Ω. The wave is propagating in an inhomogeneous piezoelectric plane with inhomogeneity direction $\alpha = \pi/2$ and different values of the normalized magnitude $rc = 0.03; 0.05; 0.08; 0.15; 0.2$. This figure presents very clear that the main idea of the multifunctional-graded material works successfully and that the magnitude and the distribution of the dangerous stress concentration fields can be reduced by controlling the properties of the graded material.

Figure 9a and b reveal the behavior of the SIF at the left crack tip K^{*L}_{III} and at the right crack tip K^{*R}_{III} in the case of the same scenario as those in Fig. 8. The concentration of the stress near the crack depends also on the properties of functional graded material, on the frequency of the applied load, and on the crack disposition according to the hole. The different behavior of the SIF at the left and at the right crack tip gives information about both phenomena hole–crack interaction and wave–graded material interaction. It is obviously that the defects' interaction should be taken into consideration at evaluation of the stress field in graded piezoelectric solids with defects of different type.

The dependence of the stress concentration field on the inhomogeneity direction of the graded material is shown in Fig. 10. Consider the hole–vertical crack configuration, see Fig. 2b, at half-distance between the hole and the crack $e = 3.5c$. The normalized frequency of the propagating SH-type wave is assigned to take two values: $\Omega = 0.5$ and $\Omega = 1.1$. The normalized magnitude of the material inhomogeneity is $rc = 0.15$. In Fig. 10a and b, SCF are displayed generalized at the observer point with $\gamma = 0$ along the circular hole. It shown the influence of both the properties of the graded piezoelectric and the characteristics of the dynamic load on the dynamic stress response near the defects. The direction of the material inhomogeneity is also an important factor for the evaluation of stress concentrations in a graded piezoelectric with defects.

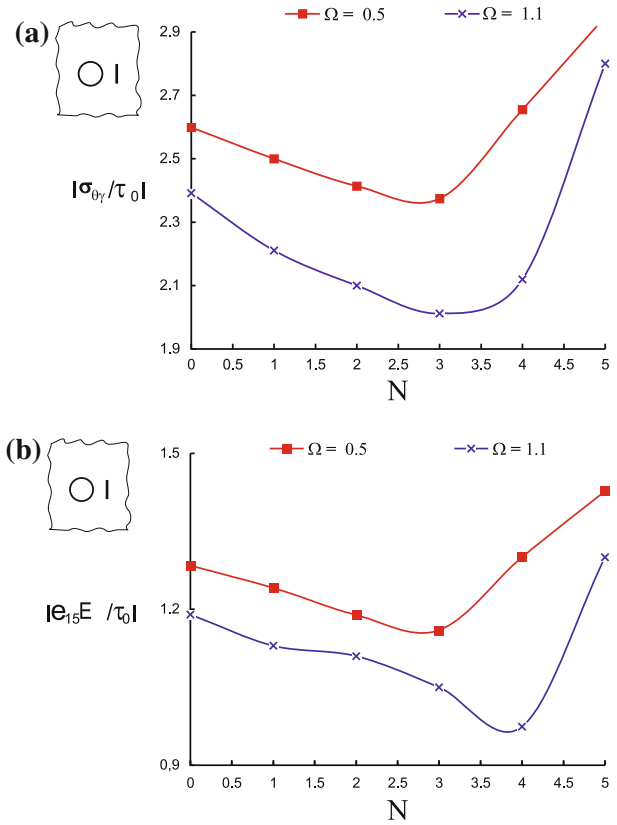

Fig. 10 Dynamic SCF versus direction of the material inhomogeneity $\alpha = N\frac{\pi}{6}$, $N \in [1, 5]$ of an inhomogeneous piezoelectric plane with a hole–vertical crack system where the magnitude of the material inhomogeneity is $rc = 0.15$, the normalized frequency is $\Omega = 0.5$ or $\Omega = 1.1$ and the half-distance between the crack and hole is $e = 3.5$: **a** and **b** mechanical and electric field SCF at observer point $\gamma = 0$

The key parameters responsible for the integrity and durability of the engineering structures made by graded PEM are the factors considered here, such as characteristics of the applied dynamic load, elastic, electric and piezoelectric properties of the material, the anisotropy and the nature of material inhomogeneity, existence of defects of different type, geometry of the defect, and their mutual position and interaction.

6 Conclusion

A two-dimensional, dynamic time-harmonic anti-plane analysis of a functionally graded piezoelectric plane with an exponential spatial variation of its material properties and weakened by a system of a crack and a hole is presented. The analysis is carried out using a non-hypersingular, traction BIEM based on the frequency-dependent fundamental solution. The BIEM formulation was numerically processed by discretizing the crack and the hole boundary with quadratic boundary elements and using standard collocation schemes. The resulting method is validated by comparing with results obtained by other computational tools. The basic problem comprising of a hole–crack system in an infinite sheet of FGPM is solved for the case of propagating SH-type waves. The results of these numerical simulations show that the stress concentration field at the crack tips and near the hole is strongly influenced by the presence of material inhomogeneity. The simulations clearly show that the dynamic stress and electric field concentrations are sensitive to different key parameters like geometry of the defects, type, and characteristics of the loading, electromechanical coupling, anisotropy, material gradient and its direction, the relation between the inhomogeneity magnitude and the defect size, the mutual hole–crack configuration, the wave–defect and wave–material interactions.

Acknowledgments The authors acknowledge the support of the Deutsche Forschungsgemeinschaft under the grant number: 436BUL 113/150/0-1 and the support of the Bulgarian National Science Fund under the grant number: DID 02/15.

References

1. Erdogan, F., Gupta, G., Ratwani, M.: Interaction between a circular inclusion and an arbitrarily oriented crack. J. Appl. Mech. T ASME **47**, 1007–1013 (1974)
2. Gharpuray, V.M., Keer, L.M., Lewis, J.L.: Cracks emanating from circular voids or elastic inclusions in pmma near a bone-implant interface. J. Biomed. Eng **112**, 22–28 (1990)
3. Wang, Y.B., Chau, K.T.: A new boundary element method for mixed boundary value problems involving cracks and holes:interactions between rigid inclusions and cracks. Int. J. Fract **110**, 387–406 (2001)
4. Hwu, C., Liang, Y.K., Yen, W.J.: Interactions between inclusions and various types of cracks. Int. J. Fract **73**, 301–323 (1995)
5. Gong, S.H., Meguid, S.A.: General-solution to the anti-plane problem of an arbitrary located elliptic hole near the tip of a main crack. Int. J. Solids Struct **28**, 249–263 (1991)
6. Liaw, B.M., Kamel, M.: A crack approaching a curvilinear hole in an anosotropic plane under general loadings. Eng. Fract. Mech **40**, 25–35 (1991)
7. Chen, Y.Z., Wang, Z.X.: Solutions of multiple crack problems of a circular region with free of fixed boundary condition in antiplane elasticity. Int. J. Fract **30**, 287–293 (1986)
8. Hasebe, N., Wang, X., Kondo, M.: Interaction between crack and arbitrary shaped hole with stress and displacement boundaries. Int. J. Fract **119**, 83–102 (2003)
9. Lu, J.F., Hanyga, A.: Dynamic interaction between multiple cracks and a circular hole swept by sh waves. Int. J. Solids Struct **41**, 6725–6744 (2004)
10. Meguid, S.A., Wang, X.D.: The dynamic interaction of a crack with a circular hole under antiplane loading. J. Mech. Phys. Solids **43**(12), 1857–1874 (1995)
11. Wang, X., Yu, S.: Scattering of sh waves by an arc-shaped crack between a cylindrical piezoelectric inclusion and matrix-ii: far fields. Int. J. Fract **100**(4), 35–40 (1999)
12. Xu, X.L., Rajapakse, R.K.N.D.: Boundary element analysis of piezoelectric solids with defects. Composit Part B: Eng **29**, 655–669 (1998)
13. Sosa, H.: Plane problems in piezoelectric media with defects. Int. J. Solids Struct **28**, 491–505 (1991)
14. Lekhnitskii, S.G.: Anisotropic plates. Gordon and Breach Science Publishers, New York (1968)
15. Liu, Y., Fan, H.: On the conventional boundary integral formulation for piezoelectric solidwith defects or thin shapes. Eng. Anal. BE **25**, 77–91 (2001)
16. Qin, Q., Mai, W.: Bem for crack-hole problems in thermopiezoelectric materials. Eng. Fract. Mech **69**, 577–588 (2002)
17. Qin, Q., Lu, M.: Bem for crack-inclusion problems of palne thermopiezoelectric solids. Int. J. Numer. Meth. Engng **40**, 1071–1088 (2000)
18. Zhou, Z.D., Zhao, S.X., Kuang, Z.B.: Stress and electric displacement analysis in piezoelectric media with an elliptic hole and a small crack. Int. J. Solids Struct **42**, 2803–2822 (2005)
19. Song, T., Li, H., Dong, J.: Dynamic anti-plane behaviour of the interaction between a crack and a circular cavity in a piezoelectric medium. Key Eng. Mater **324**(325), 29–32 (2006)
20. Dineva, P., Gross, D., Müller, R., Rangelov, T.: Biem analysis of dynamically loaded anti-plane cracks in graded piezoelectric finite solids. Int. J. Solids Struct **47**, 3150–3165 (2010)
21. Dineva, P., Gross, D., Müller, R., Rangelov, T.: Dynamic stress and electric field concentration in a functionally graded piezoelectric solid with a hole. Z. Angew. Math. Mech **91**(2), 110–124 (2011)
22. Davi, G., Milazzo, A.: Multi-domain boundary integral formulations for piezoelectric materials fracture mechanics. Int. J. Solids Struct **38**, 7065–7078 (2001)
23. Rangelov, T., Dineva, P., Gross, D.: Effect of material inhomogeneity on the dynamic behaviour of cracked piezoelectric solids: a biem approach. ZAMM - Z. Angew. Math. Mech **88**(2), 86–99 (2008)
24. Akamatsu, M., Nakamura, G.: Well-posedness of initial-boundary value problems for piezoelectric equations. Appl Anal **81**, 129–141 (2002)
25. Khutorianski, N.M., Sosa, H.: Dynamic representation formulas and fundamental solutions for piezoelectricity. Int. J. Solids Str **32**, 3307–3325 (1995)
26. Pan, E.: A bem analysis of fracture mechanics in 2d anisotropic piezoelectric solids. Engn. Anal. BE **23**, 67–76 (1999)
27. Zhang, C., Gross, D.: On wave propagation in elastic solids with cracks. Comp. Mech. Publ, Southampton (1998)
28. Wang, C-Y., Zhang, C.: 2d and 3d dynamic green's functions and time-domain bie formulations for piezoelectric solids. Engng. Anal. BE **29**, 454–465 (2005)
29. Rangelov, T., Dineva, P., Gross, D.: A hyper-singular traction boundary integral equation method for stress intensity factor computation in a finite cracked body. Engng. Anal. BE **27**, 9–21 (2003)
30. Pao, Y.H., Mow, C.C.: Diffraction of elastic waves and dynamic stress concentration. Crane Russak, New York (1971)
31. Manolis, G.D., Beskos, D.E.: Dynamic stress concentration studies by boundary integrals and laplace transform. Int. J. Numer. Meth. Eng **17**, 573–599 (1981)
32. Fang, X.Q.: Multiple scattering of electro-elastic waves from a buried cavity in a functionally graded piezoelectric material layer. Int. J. Solids Struct **45**, 5716–5729 (2008)
33. Shindo, Y., Moribayashi, H., Narita, F.: Scattering of antiplane shear waves by a circular piezoelectric inclusion embedded in a piezoelectric medium subjected to a steady-state electrical load. ZAMM, Z. Angew. Math. Mech **82**, 43–49 (2002)
34. Suo, Z., Kuo, C., Barnett, D., Willis, J.: Fracture mechanics for piezoelectric ceramics. J. Mech. Phys. Solids **40**, 739–765 (1992)
35. Wang, X.D., Meguid, S.A.: Modelling and analysis of the dynamic behaviour of piezoelectric materials containing interfacing cracks. Mech. Mater **32**, 723–737 (2000)
36. Daros, C.H.: On modelling sh-waves in a class of inhomogeneous anisotropic media via the boundary element method. ZAMM - Z. Angew. Math. Mech **90**, 113–121 (2010)